

Control of the Pump Cycle in Bacteriorhodopsin: Mechanisms Elucidated by Solid-State NMR of the D85N Mutant

Mary E. Hatcher,^{*†} Jingui G. Hu,^{*†} Marina Belenky,^{*} Peter Verdegem,[‡] Johan Lugtenburg,[‡] Robert G. Griffin,[§] and Judith Herzfeld^{*¶}

^{*}Department of Chemistry and [¶]Keck Institute for Cellular Visualization, Brandeis University, Waltham Massachusetts 02454, and

[§]Department of Chemistry and [†]Francis Bitter Magnet Laboratory, Massachusetts Institute of Technology, Cambridge, Massachusetts 02139 USA; and [‡]Rijksuniversiteit te Leiden, 2300 RA Leiden, The Netherlands

ABSTRACT By varying the pH, the D85N mutant of bacteriorhodopsin provides models for several photocycle intermediates of the wild-type protein in which D85 is protonated. At pH 10.8, NMR spectra of [ζ -¹⁵N]lys-, [12-¹³C]retinal-, and [14,15-¹³C]retinal-labeled D85N samples indicate a deprotonated, 13-*cis*,15-*anti* chromophore. On the other hand, at neutral pH, the NMR spectra of D85N show a mixture of protonated Schiff base species similar to that seen in the wild-type protein at low pH, and more complex than the two-state mixture of 13-*cis*,15-*syn*, and all-*trans* isomers found in the dark-adapted wild-type protein. These results lead to several conclusions. First, the reversible titration of order in the D85N chromophore indicates that electrostatic interactions have a major influence on events in the active site. More specifically, whereas a straight chromophore is preferred when the Schiff base and residue 85 are oppositely charged, a bent chromophore is found when both the Schiff base and residue 85 are electrically neutral, even in the dark. Thus a “bent” binding pocket is formed without photoisomerization of the chromophore. On the other hand, when photoisomerization from the straight all-*trans*,15-*anti* configuration to the bent 13-*cis*,15-*anti* does occur, reciprocal thermodynamic linkage dictates that neutralization of the SB and D85 (by proton transfer from the former to the latter) will result. Second, the similarity between the chromophore chemical shifts in D85N at alkaline pH and those found previously in the M_n intermediate of the wild-type protein indicate that the latter has a thoroughly relaxed chromophore like the subsequent N intermediate. By comparison, indications of L-like distortion are found for the chromophore of the M_o state. Thus, chromophore strain is released in the M_o→M_n transition, probably coincident with, and perhaps instrumental to, the change in the connectivity of the Schiff base from the extracellular side of the membrane to the cytoplasmic side. Because the nitrogen chemical shifts of the Schiff base indicate interaction with a hydrogen-bond donor in both M states, it is possible that a water molecule travels with the Schiff base as it switches connectivity. If so, the protein is acting as an inward-driven hydroxyl pump (analogous to halorhodopsin) rather than an outward-driven proton pump. Third, the presence of a significant C=N *syn* component in D85N at neutral pH suggests that rapid deprotonation of D85 is necessary at the end of the wild-type photocycle to avoid the generation of nonfunctional C=N *syn* species.

INTRODUCTION

Proton pumps create transmembrane electrochemical potentials that provide energy for cellular processes via ATP synthesis and coupled transport. However, the molecular mechanisms of these and other ion pumps are not understood. Bacteriorhodopsin (bR), the sole protein in the purple membrane of *Halobacterium salinarum*, is a light-driven ion pump that has been studied by a wide variety of biophysical techniques in an effort to elucidate the energy transduction mechanism (Lanyi, 1998; Haupts et al., 1999; Subramaniam, 1999; Herzfeld and Tounge, 2000). The pigment consists of a single polypeptide chain of 248 amino acids that folds into a bundle of seven transmembrane

helices. Situated in the middle of this bundle is the retinylidene chromophore formed by a Schiff base (SB) between retinal and K216. In the resting state, the SB is protonated and interacts weakly with a diffuse counterion comprising a hydrogen-bonded complex of water molecules and acidic and basic amino acid residues.

The pump cycle of bR (Fig. 1) includes at least six optically distinct intermediates (J, K, L, M, N, and O). Light absorption causes isomerization of the retinal from all-*trans* to 13-*cis* followed by a drop in the pK_a of the SB. This results in release of the SB proton during the L→M transition (microseconds). The proton acceptor, D85, is in the extracellular half of the transport channel and, if the pH of the medium is not too low, another group near the extracellular surface immediately releases a proton to the extracellular solution. (Otherwise, proton release is delayed to the end of the photocycle (Zimanyi et al., 1992; Cao et al., 1995).) In the M→N transition (milliseconds), the SB is reprotonated from D96, which is in the cytoplasmic half of the transport channel. Therefore, a switch in connectivity of the SB from the extracellular side to the cytoplasmic side must occur between the L→M and M→N transitions. In the N→O transition, D96 becomes reprotonated and the chro-

Submitted July 17, 2001, and accepted for publication October 30, 2001.

M. E. Hatcher's present address: W. M. Keck Science Center, The Claremont Colleges, Claremont, CA 91730.

J. G. Hu's present address: Materials Research Lab, University of California, Santa Barbara, CA 93106.

Address reprint requests to Dr. Judith Herzfeld, Brandeis University, Department of Chemistry MS#105, 415 South St., Waltham, MA 02454-9110. Tel.: 781-736-2538; Fax: 781-736-2516; E-mail: herzfeld@brandeis.edu.

© 2002 by the Biophysical Society

0006-3495/02/02/1017/13 \$2.00

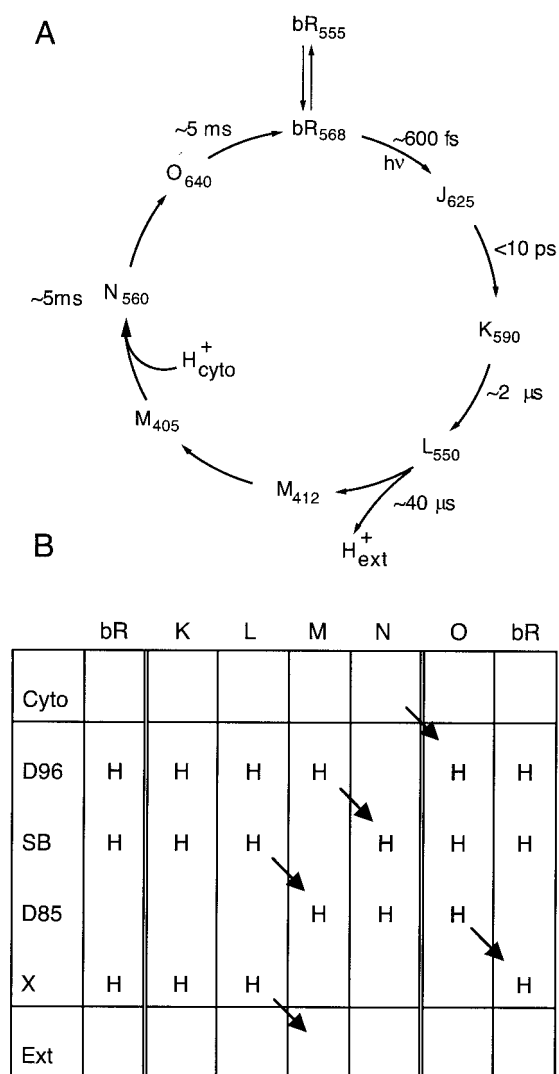


FIGURE 1 (A) The photocycle of bR₅₆₈; (B) movement of protons through the protein, from the cytoplasmic surface to the extracellular surface, during the photocycle. Double vertical lines indicate transitions with isomerization of the C₁₃=C₁₄ bond of the chromophore, first from *trans* to *cis* and then back again.

mophore reisomerizes. Finally, the deprotonated state of D85 is restored in the O→bR transition.

Although the switch in connectivity of the SB requires that there be at least two M states, distinguishing meaningfully between them has been difficult. In wild-type (WT) bR, helix movements occur during the lifetime of the M state (Dencher et al., 1989; Subramaniam et al., 1993; Han et al., 1994; Vonck et al., 1994; Sass et al., 1997). Because these changes open the cytoplasmic end of the channel, it is thought that they facilitate proton uptake. However, because the channel opening is equally effective in mutants where it occurs earlier in the photocycle (Subramaniam et al., 1999; Tittor et al., 2000), it cannot be coupled to the change in connectivity of the SB that must occur while it is deprotonated.

Understanding the switch in SB connectivity therefore requires direct probes of the active site. Solid-state NMR (SSNMR) of the chromophore in native WT bR has provided direct evidence for sequential M states in the photocycle (Hu et al., 1998). The early M state, M_o, has two substates, M_{o1} and M_{o2}, and the late M state, M_n, coexists with N. It was determined that the M_o→M_n transition involves an increase in the pK_a and/or H-bonding of the SB, as well as H-bonding changes in the peptide backbone. Recently, optical studies of native bR have also distinguished two M states. Using conditions that vary the relative lifetimes of early and late M species, it was determined that the maximum absorbance shifts from 412 nm to 405 nm during the time that the SB is deprotonated (Radionov et al., 1999).

As indicated above, Asp96 and Asp85 are central to proton translocation, Asp96 as the proton donor to the SB and Asp85 as the proton acceptor (Mogi et al., 1988). Replacement of Asp96 with non-ionizable residues slows the reprotonation of the SB (decay of M) and renders the pump bulk pH dependent (Otto et al., 1990). Replacement of Asp85 with non-ionizable residues prevents the deprotonation of the SB (formation of M) at neutral pH and renders the pump inactive except under alkaline conditions. Replacement of either of the other two internal aspartic acids, Asp212 and Asp115, with non-ionizable residues also affects the pumping efficiency, but the roles of these residues are not as well defined (Mogi et al., 1988; Otto et al., 1990; Rothschild et al., 1990; Needleman et al., 1991).

The D85N mutant of bR is uncharged at residue 85. In this respect it is similar to the M, N, and O intermediates in the WT photocycle in which D85 is protonated. UV-vis spectroscopy over a wide range of pH values showed that, unlike the resting state of WT bR, which has a λ_{max} of 568 over the range of pH 6–12, the absorption maximum in D85N shifts from 615 nm (O-like) at neutral pH, where the SB is protonated, to 405 nm (M-like) at alkaline pH, where the SB is deprotonated (Turner et al., 1993). Decomposition of absorption spectra at intermediate pH values also found a species with λ_{max} = 570 nm (N-like). Similarities between the pH-dependent states of the D85N mutant and the late intermediates of the WT photocycle also extend to large-scale structure in that raising the pH of D85N from 7 to 11 in the dark results in a change in x-ray scattering similar to that observed when the SB deprotonates in the WT photocycle (Kataoka et al., 1994).

To date, the analogies between the D85N states and the WT photocycle intermediates have been based on optical spectroscopy. However, SSNMR has also been highly successful in studies of retinal pigments (Herzfeld and Lansing, 2002; Herzfeld and Tounge, 2000; Herzfeld and Hu, 1996; Engelhard and Bechinger, 1995). Modern NMR offers a variety of measurements, but the most basic NMR probe remains the chemical shift. With its origin in the local electron distribution, the chemical shift is a sensitive re-

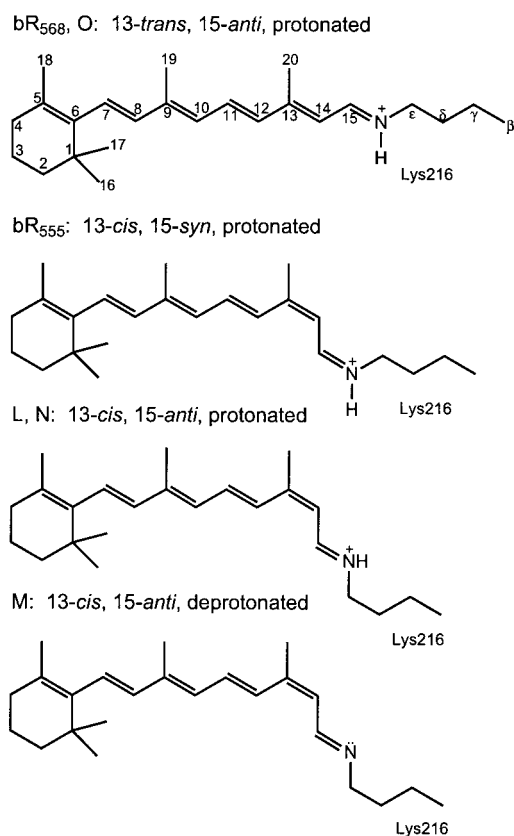


FIGURE 2 Retinal Schiff base configurations in different states of bR.

porter of the chemical environment of isotopically labeled atoms. Fig. 2 shows the various chromophore configurations adopted by bR during its photocycle. Previous workers have shown that the ^{15}N chemical shift of the SB reflects its protonation state and the strength of its interactions with surrounding groups (Harbison et al., 1983; de Groot et al. 1989; Hu et al. 1994, 1997a). ^{15}N SSNMR studies have been reported for the SB in the dark-adapted, light-adapted, L, M_o, M_n, and N states of bR as well as in the acid blue and chloride purple forms. (Harbison et al., 1983; Smith et al., 1989; de Groot et al., 1990; Lakshmi et al., 1994; Hu et al. 1997b, 1998). ^{13}C chemical shifts, on the other hand, provide probes of the isomerization state of the retinal. Through γ -effects (strong steric interactions between protons on carbons separated by three bonds), the chemical shift of C-12 provides information about the *cis/trans* isomerization of the C₁₃=C₁₄ bond and the chemical shift of C-14 provides information about the configuration of the C₁₅=N bond (Harbison et al., 1984a,b). These diagnostics have also been applied to various states of WT bR (Harbison et al., 1984a,b; Smith et al., 1989; de Groot et al., 1990; Lakshmi et al., 1994; Hu et al., 1998). In the present study, we extend these SSNMR studies to the neutral and alkaline forms of D85N and compare the results with those obtained in the WT protein. The comparison elucidates specific events in

the pump cycle, in particular, the impetus for proton transfer from the SB to D85, the decisive switch in SB connectivity from the extracellular side of the membrane to the cytoplasmic side, and the efficient recovery of a functional state at the end of the photocycle.

MATERIALS AND METHODS

Preparation of [ζ - ^{15}N]lysine D85N

The D85N-bR strain of *Halobacterium salinarum* (kindly provided by Richard Needleman) was grown in a defined medium similar to that of Gochbauer and Kushner (1969), except that the D-amino acids and NH_4Cl were omitted and the L-lysine was replaced by 0.085 g/L L- $[\zeta$ - ^{15}N]lysine. In addition, the starter cultures contained novobiocin (1 mg/ml) to select against the WT strain. The D85N-bR was isolated as is usual for WT bR (Oesterhelt and Stoekenius, 1974), taking only the densest band from the sucrose gradient.

Regeneration of D85N-bR with ^{13}C -labeled retinal

[12- ^{13}C]Retinal and [14,15- ^{13}C]retinal were synthesized as described elsewhere (Pardo et al., 1985, 1984). 120 mg of unlabeled D85N was completely bleached (colorless) by illumination of a suspension in 50 ml of 0.5 M hydroxylamine (pH 8) for 12 h with 540-nm light. The bleached sample was washed with 10 mM HEPES buffer (pH 7, room temperature) three times. A 1.1-fold molar excess of ^{13}C -labeled retinal (1.3 μM in ethanol) was added, at room temperature and in the dark, via small aliquots with vigorous shaking. The sample was stored in the dark overnight at -4°C . The regenerated sample appeared green due to the presence of excess retinal. Repeated washing (11 times) with 2% bovine serum albumin at room temperature removed this retinal. The UV-vis spectrum of the resulting bright blue sample indicated complete regeneration.

Preparation for NMR studies

D85N suspended in deionized water was washed three times with 0.3 M Gdn-HCl containing 1 mM Na_2HPO_4 at pH 10.9. (UV-vis spectra of D85N in Gdn-HCl and 1 mM Na_2HPO_4 are identical to those in NaCl and 1mM Na_2HPO_4 , both at pH 6.5 and at pH 10.9. However in Gdn-HCl at pH 10.9, the M-like state persists for the lifetime of the experiment, whereas in NaCl the sample shows the presence of a purple species within minutes under white light.) These washes were followed by 60 min of centrifugation at $30,000 \times g$, resulting in a tightly packed pellet. The pH of the supernatant of the final wash was 10.8, and the final sample color was bright yellow. The pellet was allowed to hang upside down for 4 h to release excess water. This sample was then packed into a 5-mm zirconium rotor (Chemagnetics, Fort Collins, CO) by centrifugation after each addition of material. All the washes and packing procedures were carried out in the dark to prevent photoisomerization. After the spectra at pH 10.8 had been obtained, the sample was unpacked and washed three times in 300 mM Gdn-HCl solution 1 mM Na_2HPO_4 at pH 6.5. The pH of the final supernatant was 6.5, and the sample was bright blue in color. This sample was repacked in the same manner as above.

Low-temperature solid-state NMR

All spectra were obtained on a custom-built spectrometer with a proton frequency of 317 MHz (79.9 MHz for ^{13}C and 32.2 MHz for ^{15}N), using a custom-built, four-channel, variable-temperature, transmission line probe designed and fabricated by J. G. Hu and C. M. Rienstra. The spectra were recorded at -100°C to improve the signal-to-noise ratio. A ramped cross-

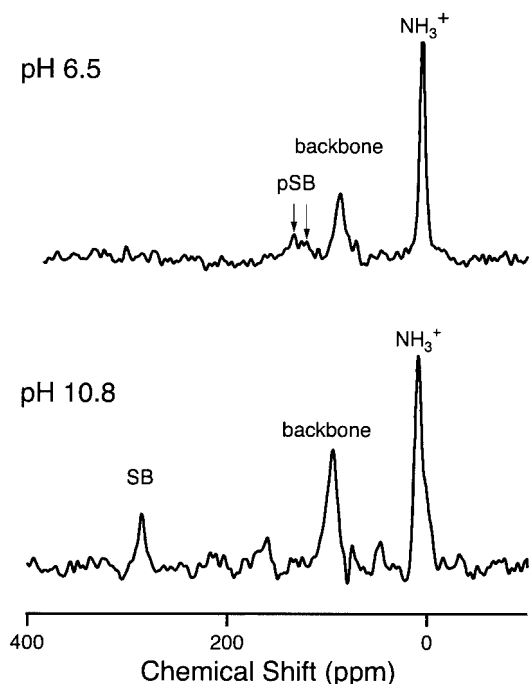


FIGURE 3 The ^{15}N MAS ($\omega_r/2\pi = 5.0$ kHz) spectra of $[\zeta\text{-}^{15}\text{N}]\text{lys-D85N}$ at pH 6.5 and pH 10.8. The two upfield peaks correspond to the signals of the free lysines and the natural abundance signal of the peptide backbone. The Schiff base nitrogen resonance is a broad peak at pH 6.5 (arrows indicate range from 128 ppm to 142 ppm) and a narrow peak at 286 ppm at pH 10.8.

polarization pulse sequence, two pulse phase modulation (TPPM) decoupling (Bennett et al., 1994), and a recycle delay of 3 s were used. Typically, the proton 90° pulse was $2.5 \mu\text{s}$, the cross-polarization period was 2 ms, the decoupling power was 100 kHz, and the spinning frequency was 5.0 kHz. The spectra were acquired for 20 h, resulting in 35,000–40,000 transients. The ^{13}C chemical shifts were referenced to tetramethylsilane (TMS), and the ^{15}N chemical shifts were referenced to saturated (5.6 M) $^{15}\text{NH}_4\text{Cl}$ (which is 26.9 ppm downfield from the signal of liquid ammonia). Internal references were the ^{13}C shift of the peptide backbone at 173 ppm and the ^{15}N shift of the free lysine residues at 8.4 ppm. The ^{13}C spectra were simplified by removing the natural abundance background using difference spectroscopy techniques described previously (de Groot et al., 1988).

RESULTS

$[\zeta\text{-}^{15}\text{N}]\text{Lys-D85N-bR}$

The ^{15}N CPMAS spectra of $[\zeta\text{-}^{15}\text{N}]\text{lys-D85N-bR}$ at alkaline and neutral pH are shown in Fig. 3. The resonances at 8.4 ppm and 93.6 ppm are due to the natural abundance signals of the free lysines and the peptide backbone, respectively, whereas the downfield resonances are due to the SB.

The most distinctive feature in Fig. 3 is the appearance of a relatively sharp peak at 286 ppm in the pH 10.8 sample. This chemical shift is almost identical to that found for the M_n state of WT bR (Hu et al., 1998). The sharpness of the peak at 286 ppm suggests the presence of a single deprotonated SB species. Upfield resonances typical of protonated

retinal Schiff bases are not present in the pH 10.8 preparation of D85N. This was achieved by the use of guanidine hydrochloride (Gdn-HCl), which retards the reprotonation of the SB (Yoshida et al., 1980). In contrast, UV-vis studies of D85N in NaCl show coexistence of an N-like (570 nm) component at this pH (Turner et al., 1993; Dickopf et al., 1995). (The N-like state was not studied because it appears only in mixtures, resulting in poor signal-to-noise for all the species present.)

At pH 6.5, the broad envelope of peaks centered at 133 ppm indicates multiple protonated SB species. It has been shown previously that the ^{15}N chemical shift of the protonated SB is very sensitive to the counterion environment, exhibiting an upfield trend for systems with weaker counterion interactions (Harbison et al., 1983; de Groot et al., 1989; Hu et al., 1994, 1997a). The upfield shift of the D85N protonated SB relative to WT bR is consistent with a weakened counterion in D85N, as expected when the D85 charge has been removed.

$[12\text{-}^{13}\text{C}]\text{Retinylidene-D85N-bR}$

The ^{13}C CPMAS spectra of $[12\text{-}^{13}\text{C}]\text{retinylidene D85N}$ for neutral (pH 6.5) and alkaline (pH 10.8) conditions are shown in Figs. 4 A and 5 A, respectively. The peaks at 173 ppm and 126 ppm are the natural abundance signals of the carbonyl and aromatic carbons, respectively. The peak at 156 ppm is due to guanidyl carbons as it exists in samples washed in NaCl or Gdn-HCl, but the intensity is greater in those washed in Gdn-HCl. Figs. 4 B and 5 B show the ^{13}C spectra of natural abundance bR at the same temperature and spinning speed as for the retinal-labeled D85N. In each case, subtraction of the spectrum of the natural abundance sample from the spectrum of the labeled sample isolates the signals from the retinal labels alone (Figs. 4 C and 5 C).

At pH 10.8, the difference spectrum (Fig. 5 C) shows a single $12\text{-}^{13}\text{C}$ peak at 122 ppm. This represents a 13-*cis* species that we know from the ^{15}N spectra contains a deprotonated SB. Both features are consistent with an M-like state. As in the ^{15}N spectra, the peak at 122 ppm is narrow, suggesting the presence of a single M-like species at this pH.

At pH 6.5, the difference spectrum (Fig. 4 C) shows a multiplet of resonances centered at 131 ppm and 122 ppm. Signals centered around 131 ppm are due to retinal in the all-*trans* state, whereas signals centered around 122 ppm are due to 13-*cis* retinal. This difference in chemical shift is due to steric interaction between the protons on C-12 and C-15 of the retinal (Harbison et al., 1984a,b). The relative intensities of the peaks suggest that the 13-*cis* and all-*trans* species are present in similar quantities. The resolution of the 131- and 122-ppm peaks indicates that, at -100°C , the rate for 13-*cis*/all-*trans* interconversion is much less than 720 s^{-1} . The breadth of the 131-ppm peak indicates that the all-*trans* state is considerably disordered. This may reflect

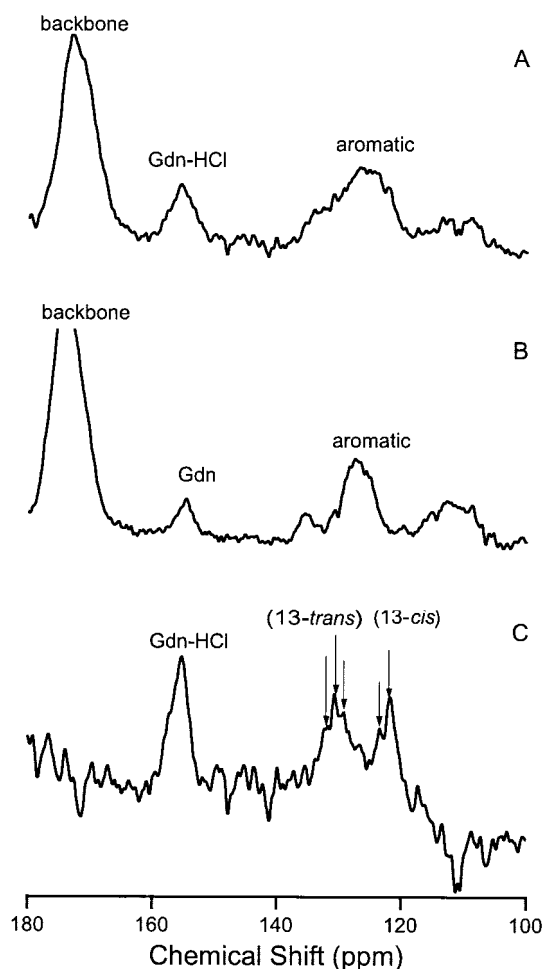


FIGURE 4 Downfield region of the ^{13}C MAS ($\omega_r/2\pi = 5.0$ kHz) spectra of $[12\text{-}^{13}\text{C}]$ retinylidene-D85N at pH 6.5 (A), natural abundance bR (B), and their difference (C). The natural abundance peaks from the peptide backbone, aromatic residues, and Gdn-HCl are labeled. The arrows indicate the 122.2-ppm and 124.0-ppm resonances of the 13-*cis* species and the 129.2-, 130.7-, and 132.0-ppm resonances of the 13-*trans* species present in D85N^{neut}. The negative feature upfield from the C_{12} resonances in the difference spectrum is from the spinning sideband of the backbone resonance. This incomplete subtraction arises from an imperfect match of the CP conditions between the backbone regions of the $[12\text{-}^{13}\text{C}]$ retinylidene-D85N and the unlabeled bR spectra.

variations elsewhere in the chromophore or in the surrounding protein.

[14,15- ^{13}C]Retinylidene-D85N-bR

The ^{13}C CPMAS spectra of $[14,15\text{-}^{13}\text{C}]$ retinylidene D85N for pH 6.5 and pH 10.8 are shown in Figs. 6 A and 7 A, respectively. Again, the peaks at 173 ppm and 126 ppm are the natural abundance signals of the carbonyl and aromatic carbons, respectively, whereas the peak at 156 ppm is from the guanidyl carbons of the arginines in the protein and the Gdn-HCl. Figs. 6 B and 7 B show natural abundance bR spectra taken at the same temperature and spinning fre-

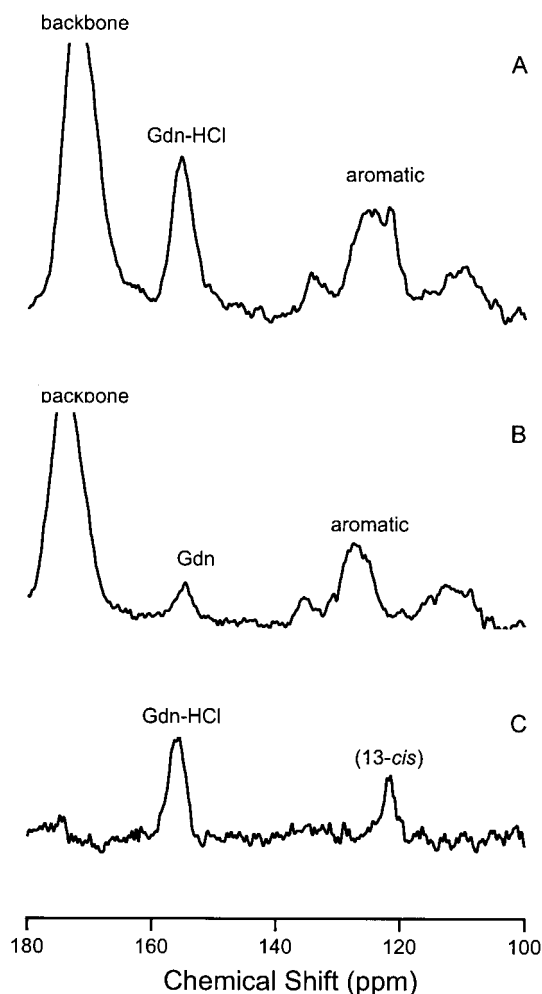


FIGURE 5 Downfield region of the ^{13}C MAS ($\omega_r/2\pi = 5.0$ kHz) spectra of $[12\text{-}^{13}\text{C}]$ retinylidene-D85N at pH 10.8 (A), natural abundance bR (B), and their difference (C). The natural abundance peaks from the peptide backbone, aromatic residues, and Gdn-HCl are labeled. The single peak at 122 ppm indicates the presence of a single 13-*cis* species in D85N^{alk}.

quency as for the retinal-labeled D85N. The difference spectra, showing the labeled retinal peaks, are found in Figs. 6 C and 7 C. It is impossible to resolve the resonances from the C-15 retinal label as they fall in the same position as the guanidyl carbon of the Gdn-HCl. However, the C-14 resonance, which we can isolate, is the signal that is diagnostic for the C=N configuration. Therefore, all further discussion about this sample will be limited to the C-14 resonances.

At pH 10.8 (Fig. 7 C), a single, narrow ^{13}C resonance is observed at 123.2 ppm, consistent with a single species as indicated by the ^{15}N and $^{12}\text{-}^{13}\text{C}$ signals. In contrast, at pH 6.5 the difference spectrum (Fig. 6 C) shows weak, broad resonances at ~ 118 and 108 ppm. These are the expected chemical shifts for 15-*anti* and 15-*syn* configurations, respectively. The signal-to-noise of these resonances is poor because the signal is dispersed over multiple species, con-

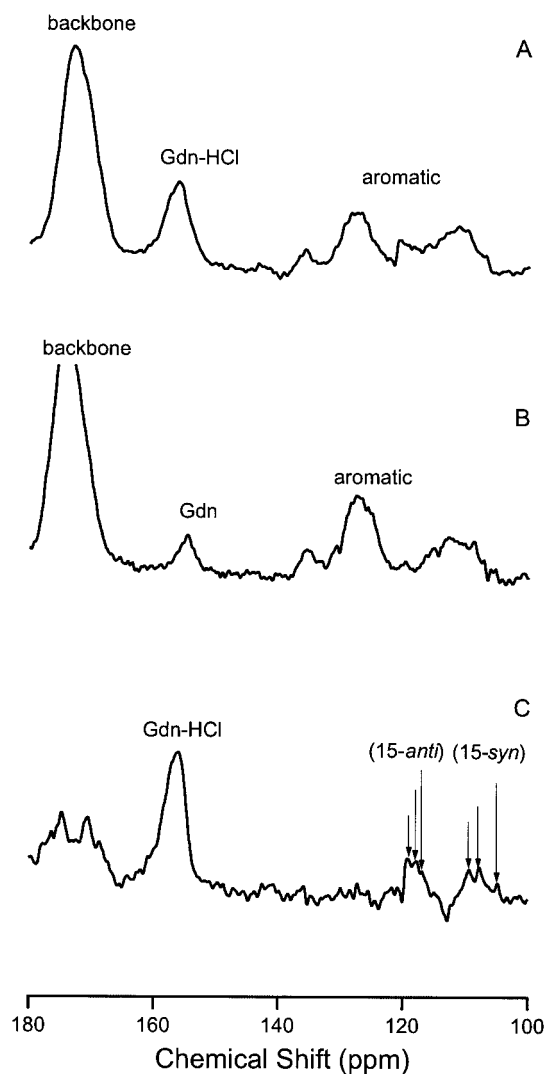


FIGURE 6 Downfield region of the ^{13}C MAS ($\omega_r/2\pi = 5.0$ kHz) spectra of $[14,15\text{-}^{13}\text{C}]$ retinylidene-D85N at pH 6.5 (A), natural abundance bR (B), and their difference (C). The natural abundance peaks from the peptide backbone, aromatic residues, and Gdn-HCl are labeled. The arrows indicate 15-*syn* species with resonances at 105.4 ppm, 108.0 ppm, and 109.3 ppm, and 15-*anti* species with resonances at 117.2 ppm, 117.9 ppm, and 119.1 ppm. The incomplete subtraction evident in the region just downfield of the Gdn-HCl resonance is caused by an imperfect match of the CP conditions in the backbone regions of the $[14,15\text{-}^{13}\text{C}]$ retinylidene-D85N and the natural abundance bR. Because we are interested in resonances near the aromatic region, the two spectra were scaled with respect to the aromatic regions.

sistent with the 12- ^{13}C signals at this pH. Again, this may reflect variations elsewhere in the chromophore or in the surrounding protein.

DISCUSSION

The newly measured chemical shifts for D85N are compared in Tables 1–3 with the corresponding shifts for various forms of WT bR. Our ^{15}N NMR results confirm that the

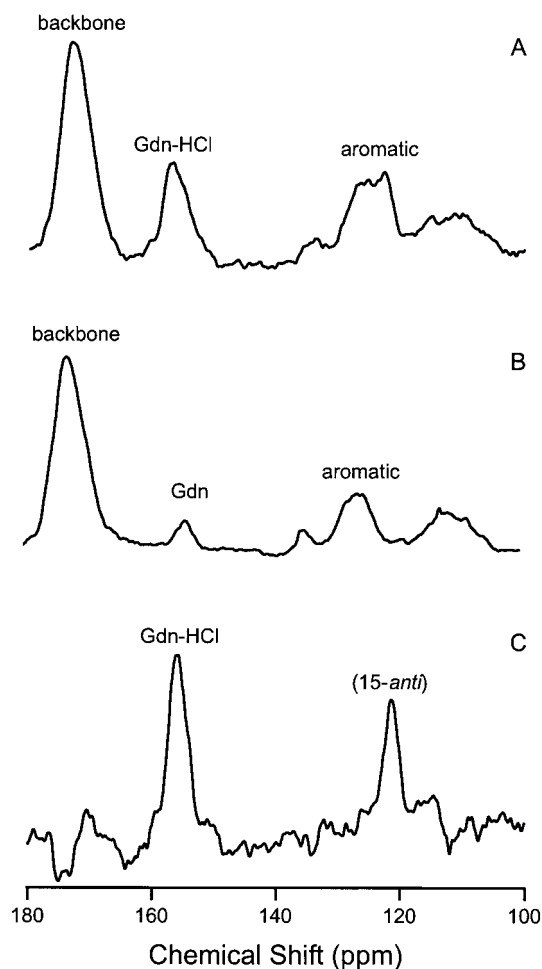


FIGURE 7 Downfield region of the ^{13}C MAS ($\omega_r/2\pi = 5.0$ kHz) spectra of $[14,15\text{-}^{13}\text{C}]$ retinylidene-D85N at pH 10.8 (A), natural abundance bR (B), and their difference (C). The natural abundance peaks from the peptide backbone, aromatic residues, and Gdn-HCl are labeled. The single peak at 123 ppm indicates the presence of a single 15-*anti* species in D85N^{alk}.

SB of D85N is protonated at pH 6.5 and deprotonated at pH 10.8. In addition, ^{13}C NMR finds only a 13-*cis*,15-*anti* chromophore configuration at pH 10.8, whereas multiple $\text{C}_{13}=\text{C}_{14}$ and $\text{C}=\text{N}$ configurations are found at pH 6.5. The finding of a mixture of all-*trans* and 13-*cis* chromophores at neutral pH confirms the conclusions of earlier extraction results (Turner et al., 1993; Marti et al., 1991; Song et al., 1995; Brown et al., 1997). However, in addition to the two $\text{C}_{13}=\text{C}_{14}$ isomers, we find that there are roughly equal populations of $\text{C}=\text{N}$ *syn* and *anti* isomers.

A mix of $\text{C}_{13}=\text{C}_{14}$ and $\text{C}=\text{N}$ configurations is also found in dark-adapted WT bR. However, in D85N^{neut}, each configuration shows considerable disorder. Whether this is due to variations in other parts of the chromophore or in the surrounding protein, there are clearly many more species present in D85N^{neut} than in WT bR under similar conditions. This exaggerated heterogeneity may account for the accessibility of the SB from both sides of the membrane

TABLE 1 ^{15}N chemical shifts of protonated (p) and nonprotonated (np) Schiff bases in [ζ - ^{15}N]lys-labeled bR

	pSB	npSB
bR ₅₆₈ (light-adapted, neutral WT)	143.5*	
bR ₅₅₅ (dark-adapted, neutral WT)	150.6 [†]	
bR ₆₀₀ (acid blue WT)	134.4, 127.3*	
bR ₅₅₅ (chloride purple WT)	147.6*	
L (WT)	161.0 [‡]	
M _o (WT)		296.4 [§]
M _n (WT)		288.8 [§]
N (WT)	150.7	
D85N ^{neut}	128.0–145.0 [#]	
D85N ^{alk}		286.2 [#]

Chemical shifts are relative to saturated (5.6 M) $^{15}\text{NH}_4\text{Cl}$ (which is 26.9 ppm downfield from the signal of liquid ammonia).

*From de Groot et al., 1990.

[†]From Harbison et al., 1983.

[‡]From Hu et al., 1997b.

[§]From Hu et al., 1998.

^{||}From Lakshmi et al., 1994.

[#]From this work.

(“flickering”) that has been found in D85N^{neut} (Brown et al., 1998). In contrast, in the M states of WT bR, and in the M_n-like D85N^{alk}, the chromophores are well ordered, as necessary for controlled access to the two sides of the membrane.

Electrostatic control in the active site

X-ray diffraction studies have found that a large-scale conformational change similar to that occurring in the WT

TABLE 2 [$^{12}\text{-}^{13}\text{C}$]Retinal chemical shifts in bR and model compounds

	All-trans	13-cis
bR ₅₆₈ (light-adapted, neutral WT)	134.3* [†]	
bR ₅₅₅ (dark adapted WT)		124.2* [†]
bR ₆₀₀ (acid blue WT)	133.5 [‡]	123.9 [‡]
6-s-cis, all-trans-retinylidenebutylimmonium chloride	135.0 [§]	
6-s-cis, 13-cis-retinylidenebutylimmonium chloride		125.1 [§]
M _o (WT)		125.7
M _n (WT)		124.5
N (WT)		124.4
D85N ^{neut}	129.2, 131.0 [#]	122.2, 124.0 [#]
D85N ^{alk}		122.0 [#]

Chemical shifts are relative to tetramethylsilane (TMS).

*From Harbison et al., 1984a.

[†]From Smith et al., 1989.

[‡]From DeGroot et al., 1990.

[§]From Harbison et al., 1985.

^{||}From Hu et al., 1998.

^{||}From Lakshmi et al., 1994.

[#]From this work.

TABLE 3 [$^{14}\text{-}^{13}\text{C}$]Retinal chemical shifts in bR

	15-syn	15-anti
bR ₅₆₈ (light-adapted, neutral WT)		122.3* [†]
bR ₅₅₅ (dark-adapted, neutral WT)	110.7* [†]	
bR ₅₆₅ (chloride purple WT)		119.7 [‡]
bR ₆₀₀ (acid blue WT)	109.8 [‡]	121.1 [‡]
M _o (WT)		123.2, 125.0 [§]
M _n (WT)		124.6 [§]
N (WT)		115.0
D85N ^{neut}	105.4, 108.0, 109.3 [#]	117.2, 117.9, 119.1 [#]
D85N ^{alk}		123.2 [#]

Chemical shifts are relative to tetramethylsilane (TMS).

*From Harbison et al., 1984b.

[†]From Smith et al., 1989.

[‡]From DeGroot et al., 1990.

[§]From Hu et al., 1998.

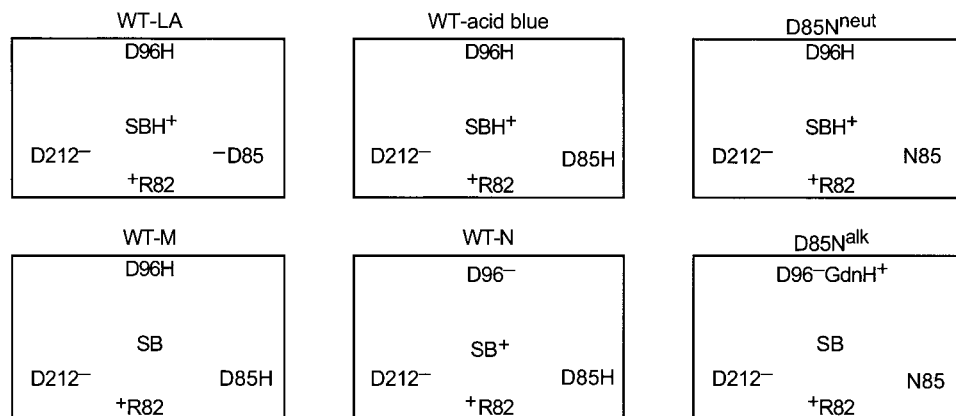
^{||}From Lakshmi et al., 1994.

[#]From this work.

photocycle can be induced either by titration of D85N from neutral to alkaline pH or by further mutation of D85N to D85N/D96N at neutral pH (Kataoka et al., 1994). Interestingly, FT-Raman indicates that the difference in tertiary structure in the latter case (between D85N and D85N/D96N at neutral pH) is not associated with a significant effect on chromophore conformation (Brown et al., 1997). Thus we expect that the similar tertiary structure change induced by pH titration of D85N would also have little effect on the chromophore. It follows that the dramatic, reversible tightening of the chromophore structure that we observe by SSNMR has more to do with the pH-induced change in the charge of the SB than with the pH-induced change in the tertiary conformation of the protein. This is consistent with the important role of electrostatic interactions in the active site that has been noted in theoretical calculations (Zhou et al., 1993; Scharnagle et al., 1995; Herome and Kuczera, 1998).

The influence of the SB charge may be via either repulsive or attractive interactions with other nearby charges. D212 (one helix turn away from the chromophore at K216) has been suggested to play an important yet undefined role in the bR photocycle (Moltke et al., 1995a,b) and happens to be the only charged residue near the SB in D85N. However, the multiplicity of chromophore configurations observed in D85N^{neut} suggests that this electrostatic interaction is not decisive. On the other hand, at high pH, where the SB has no charge, other interactions apparently snap the system into a well-defined state. The key may be wider charge balance. Fig. 8 shows the states of ionizable residues inside the transport channel for various bR species that have been studied by NMR. The ones with charge imbalance are D85N^{neut} and WT acid blue. These are also the ones with the most disordered chromophores. The present results allow a detailed comparison between these two states.

FIGURE 8 Ionizable residues inside the transport channel for various bR species that have been examined by NMR. Species in the top row are stable at neutral and low pH where D96 is protonated. Species in the bottom row are studied at high pH where D96 is deprotonated and stabilized with guanidinium ion as needed (i.e., when the SB is deprotonated).



The solid-state ^{15}N NMR spectra of WT acid blue [ζ - ^{15}N]lys-bR shows an upfield shift of the SB resonance (de Groot et al., 1990). This indicates a weaker interaction with the complex counterion, consistent with protonation of D85 and the red-shifted visible spectrum. In addition, the SB resonance is broad, indicating a range of interaction strengths, as expected for varying spatial arrangements. The resulting ^{15}N spectrum is similar to the present ^{15}N spectrum for D85N^{neut}, in which the charge from Asp85 has been removed by mutation rather than acidification (Fig. 3).

The ^{13}C NMR spectrum of WT acid blue [^{13}C]retinylidene-bR indicates a mixture of 13-*cis* and 13-*trans* species (de Groot et al., 1990) consistent with the results of resonance Raman studies (Smith and Mathies, 1985). The present spectrum of [^{13}C]retinylidene-D85N^{neut} also indicates the presence of both 13-*cis* and all-*trans* species (Fig. 5). As for acid blue bR, the all-*trans* peak is broader, suggesting greater heterogeneity than for the 13-*cis* species.

The ^{13}C NMR spectrum of WT acid blue [^{14}C]retinylidene-bR shows signals centered around 108 ppm, representing the 15-*syn* isomer, and 118 ppm, representing the 15-*anti* isomer (de Groot et al., 1990). The details of this spectrum suggest a mixture containing two 15-*syn* species and two 15-*anti* species (in contrast to the single species of each type observed in dark-adapted purple membrane). Our results for [^{14}C]retinylidene-D85N^{neut} also show *syn* and *anti* isomers, with at least two species of each (Fig. 7).

Recovery of the pump cycle

The motivation for studying D85N^{neut} was as an alternative to acid blue bR for a model of the O intermediate of the WT-bR photocycle. In all three (O, acid blue, and D85N^{neut}), the charge on D85 has been neutralized and the SB and D96 are protonated. D85N^{neut} differs from the others in H-bonding capability because it contains a -NH₂ group instead of a -OH group at residue 85. However, acid blue differs from the others in the protonation of other carboxyl groups. This effect is seen in photovoltage exper-

iments (Moltke et al., 1995a,b); the measurements of D85N between pH 6.5 and 8.5 correlate well with those of acid blue bR except for a pair of additional charge displacements at 60 μs and 1.3 ms. Therefore, in these experiments D85N^{neut} appears to be a mixture of an acid blue-like species and a second species with a transient charge transfer process. As expected, these additional charge displacements disappear in D85N as the pH is lowered. In fact, at pH 1.0, the photovoltage measurements of D85N in the absence of chloride ions are the same as for the WT acid blue bR. In addition, like WT acid blue bR, D85N at low pH turns purple upon the addition of chloride anions and its photovoltage measurements then resemble those of chloride purple bR (Moltke et al., 1995a,b).

The present results indicate that differences between D85N^{neut} and acid blue bR have little effect on the chromophore because the mixtures of chromophore configurations in the two species are very similar. Yet, the similarity of either of these species to the O intermediate is limited. On the one hand, the remarkably high energy and entropy of the O intermediate (Ludmann et al., 1998) is consistent with electrostatic imbalance and disorder in the active site. Distortion of the chromophore has also been detected by resonance Raman spectroscopy (Smith et al., 1983). On the other hand, the resonance Raman spectrum of O is sufficiently similar to that of bR₅₆₈ that it has been concluded that the chromophore is 13-*trans*,15-*anti* (Smith et al., 1985), whereas the N photocycle intermediate is 13-*cis*,15-*anti* (Fodor et al., 1988a). In contrast, we find both *cis* and *trans* C₁₃=C₁₄ configurations and both *syn* and *anti* C=C=N configurations in both D85N^{neut} and acid blue bR.

The mixture of C₁₃=C₁₄ configurations is relatively easy to reconcile with the late photocycle of WT bR. The N→O transition involves D96 reprotonation (which dominates the change in the absorption spectrum), as well as 13-*cis*/all-*trans* isomerization, and there is no reason to think that these two events are perfectly synchronous. Indeed, isomerization will occur more readily if D96 reprotonates first to give a strongly red-shifted state. If reprotonation occurs

first, then a 13-*cis* optically O-like state occurs, however briefly, in addition to the all-*trans* optically O-like state. In fact, analyses of time-resolved optical spectra indicate that the N and O states are in equilibrium during the photocycle, reflecting rapid proton dynamics at D96 (Chizhov et al., 1996; Ludmann et al., 1998). Furthermore, the balance between N and O shifts to the left with increasing pH. An analogous pH dependence is seen for the N-like and O-like states of D85N, despite the mixture of C₁₃=C₁₄ configurations in the latter.

The relationship between D85N^{neut} and the photocycle of WT bR would seem to become more distant when we consider the C=N configuration. In particular, the presence of C=N *syn* states in D85N^{neut} has no known parallel in any of the WT photocycle intermediates although it occurs in the dark-adapted state. Thus, although D85N^{neut} and O are both disordered states, there is greater C=N heterogeneity in D85N^{neut} than in O. We conjecture that the difference is probably one of time. In WT bR, D85 deprotonates at the end of the photocycle and the resulting blue-shift of the chromophore will slow down further isomerization. In addition, the renewed interaction of the protonated SB with its counterion will constrain the chromophore so that the only isomerization that occurs is the slow double isomerization, from all-*trans*,15-*syn* to 13-*cis*,15-*anti*, that is associated with dark adaptation. In contrast, the chromophore in D85N remains red-shifted and without electrostatic constraint. The comparison suggests that prompt deprotonation of D85 at the end of the WT photocycle is critical to prevent disordering of the SB linkage and maintain the efficiency of the pump.

Chromophore discharge in the pump cycle

For D85N^{alk}, our combined ¹⁵N and ¹³C NMR results demonstrate an exclusively 13-*cis*,15-*anti* chromophore with a deprotonated SB in D85N^{alk} as in the M intermediate of the WT photocycle. This order is striking compared not only with the mix of isomers found in D85N^{neut}, but also with the mix of 13-*cis*,15-*syn* and 13-*trans*,15-*anti* found in dark-adapted WT bR at both neutral and alkaline pH. For dark-adapted WT bR, it has been argued that the 13-*cis*,15-*syn* and 13-*trans*,15-*anti* species coexist because both are straight enough to fit in the same binding pocket. By contrast, the active site of D85N^{alk} clearly favors a bent chromophore. In the past, a change to an effectively bent binding pocket has been proposed to be sterically induced during the pump cycle of WT bR by photoisomerization of the chromophore from all-*trans*,15-*anti* to 13-*cis*,15-*anti* (Fodor et al., 1988a). But the results for D85N^{alk} show that all that is necessary to produce an effectively bent binding pocket is neutralization of both the SB and D85. This result is consonant with the photocycle dynamics of WT bR: because neutralization of both the SB and D85 favors a 13-*cis*,15-*anti* chromophore, it follows by reciprocal thermodynamic

linkage that a 13-*cis*,15-*anti* chromophore promotes coordinated neutralization of the SB and D85 (as occurs by proton transfer during the L→M transition of the photocycle). Structurally, this is not surprising. Isomerization from all-*trans*,15-*anti* to fully 13-*cis*,15-*anti* causes the SB to be rotated away from its complex counterion, a movement that is expected to be costly in terms of Coulomb energy until proton transfer neutralizes the SB and D85. In fact, in the L state the chromophore is strained and the SB interacts strongly with its counterion (Hu et al., 1997b). This suggests that formation of a fully 13-*cis*,15-*anti* configuration is resisted until proton transfer occurs (Herzfeld and Tounge, 2000).

The connectivity switch in the pump cycle

Recent studies have demonstrated the existence of two M photocycle intermediates in WT bR (both 13-*cis*,15-*anti*) that differ substantially in the ¹⁵N chemical shifts of the SB and slightly in the ¹³C chemical shifts of the C-12 and C-14 carbons of the retinal (Hu et al., 1998). In D85N^{alk}, the ¹⁵N chemical shift is identical to that of the late M photocycle intermediate studied by SSNMR (M_n). This is consistent with the fact that the 405-nm λ_{max} of D85N^{alk} is identical to the λ_{max} of late M in the WT photocycle (Radionov et al., 1999). The agreement suggests that the chromophores in both samples have had the opportunity to thoroughly relax after deprotonation of the SB.

Comparing different photocycle intermediates, optical spectroscopy suggests that the early M state is very similar to the late M state, and the L state is very similar to the N state. But the ¹⁵N chemical shifts of the SB indicate that the interactions of the SB are substantially different in N versus L and in late M (M_n) versus early M (M_o). In fact, as shown in Fig. 9, both L and M_o are significantly and similarly red-shifted compared with the visible absorption that would be expected according to the strength of the SB interactions indicated by their ¹⁵N chemical shifts. Thus the M_o state would seem to have preserved an important characteristic of the L state (Hu et al., 1997b) and is probably a very early, and almost certainly pre-switch, M state.

To understand the visible spectra of L and M_o in light of the SB interactions revealed by their ¹⁵N chemical shifts, we have to consider the rest of the chromophore. It is well known that twisting of the polyene chain will shift the visible spectrum, and vibrational spectroscopists have repeatedly found evidence of chromophore distortion in the first half of the photocycle. Thus the present results are consistent with those from vibrational spectroscopy. But the present results provide further information. Chromophore distortions can result in either blue-shifts or red-shifts. Torsional strain in the nominal single bonds moves the ground and excited states farther apart (resulting in a blue-shift), whereas torsional strain in the nominal double bonds moves them closer together (resulting in a red-shift). Thus the

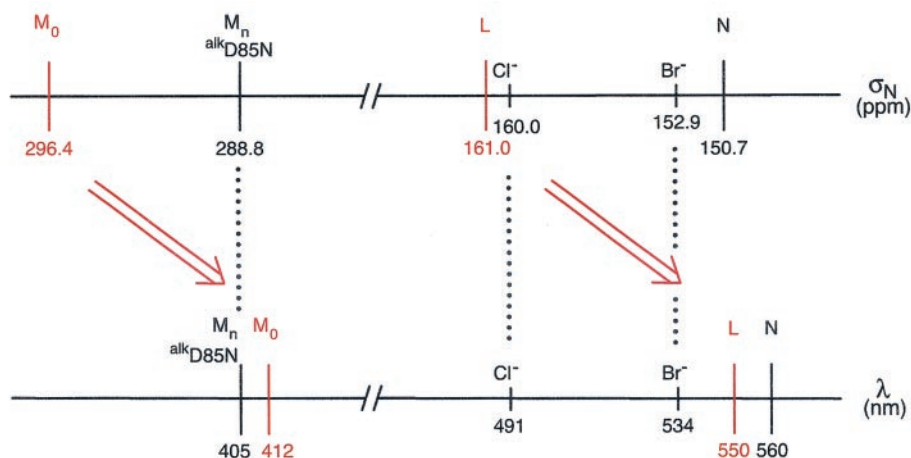


FIGURE 9 Comparison of ^{15}N chemical shifts and wavelengths of maximum visible absorbance for 13-*cis*-retinylidenes in WT bR and model compounds. The alignment of the scales (*dotted lines*) was based on the relaxed models: D85N^{alk} with an unprotonated SB (the present work) and the chloride and bromide salts of the protonated SB of retinal with aniline (Hu et al., 1997a). The ^{15}N chemical shifts for the photocycle intermediates of WT bR are from Table 1. By comparison with the models, the M_n and N chromophores are essentially relaxed, whereas the L and M_o chromophores are significantly strained as described in the text.

combination of visible and SSNMR spectroscopy suggests that in both the L and M_o states there is double bond strain that dissipates in the formation of the M_n and N states. This unwinding of the chromophore in the $M_o \rightarrow M_n$ transition may form the basis for the connectivity switch that is critical for active transport.

The idea that chromophore distortions could be at the heart of the pump mechanism was proposed earlier by Schulten and Tavan (1978). However, they focused on the nominal single bond closest to the SB, and subsequent resonance Raman and ^{13}C SSNMR results indicate that twisting around this bond is not responsible for the connectivity switch (Fodor et al., 1988b; Mathies and Li, 1995; Lansing et al., 2002). The present ^{15}N SSNMR results affirm the importance of chromophore distortion but suggest that it is the nominal double bonds that are most active in the connectivity switch.

The usefulness of torsion-driven reorientation of the SB depends on changes in the interactions of the SB. As previously noted (Hu et al., 1998), the nitrogen chemical shifts indicate that the SB in M_n is more strongly hydrogen bonded than the SB in M_o . However, even in M_o the shift of the SB nitrogen is ~ 20 ppm upfield relative to that in retinylidene butylamine (Harbison et al., 1983). This suggests that there is significant interaction with a hydrogen bond donor in the M_o state, as well as in the M_n state. A similar conclusion can be drawn from the λ_{max} values of these states (Gat and Sheves, 1994). There are then two possibilities: either the SB switches from one hydrogen bond partner to another as the chromophore unwinds or else it carries its hydrogen-bonding partner with it. The latter would require a mobile hydrogen bond donor such as water. One of the distinctive features of the active site in bR is the

presence of several water molecules. With the SSNMR and UV-vis evidence for hydrogen bonding of the SB in both the early and late M states, it is not farfetched to suppose that a water molecule remains associated with the SB as the chromophore unwinds. If this is the case, bR acts as an inward-driven hydroxide pump rather than as an outward-driven proton pump, as has recently been proposed by analogy with halide transport in halorhodopsin (Betancourt and Glaeser, 2000). Such a scenario is consistent with crystallographic evidence for rearrangement of water molecules during the photocycle (Luecke, 2000). It would also explain the presence of relatively strong SB counterions in the L and N states (Hu et al., 1997b; Lakshmi et al., 1994).

CONCLUSIONS

The present SSNMR study shows that D85N^{alk} contains a single deprotonated 13-*cis*,15-*anti* species. The absence of any straight isomers in D85N^{alk} indicates that with neutralization of D85 and the SB, the active site strongly favors a bent chromophore rather than simply accommodating one. The corollary, from reciprocal thermodynamic linkage, is that the bent chromophore produced by photoisomerization in the WT photocycle favors the proton transfer that neutralizes both the SB and D85 in the $L \rightarrow M$ transition.

Based on chemical shift measurements and visible spectroscopy, D85N^{alk} closely resembles the late M photocycle intermediate in bR. This indicates that the chromophore of the late M state, like that of the N state, is thoroughly relaxed. By comparison, the chromophore of the early M state shows signs of distortion similar to that in the L state. Thus the chromophore strain characteristic of the early

photocycle intermediates is apparently released while the SB is deprotonated. This behavior points to a pump mechanism in which the protonated SB is entrained by electrostatic interactions in the active site such that the connectivity to the extracellular medium is sustained after photoisomerization at the expense of distortions of the chromophore (Herzfeld and Tounge, 2000). Once the electrostatic interactions are released by proton transfer, the chromophore is free to unwind, resulting in a timely and decisive change in SB connectivity.

This robust mechanism is consistent with a wide variety of data. Over the years, studies of bacteriorhodopsin mutants and analogues have shown that pumping occurs even when 1) the chromophore is not covalently linked to the peptide backbone (Friedman et al., 1994, Schweiger et al., 1994), 2) there is no large-scale conformational change in the protein (Subramaniam et al., 1999; Tittor et al., 2000), 3) proton release is delayed to the end of the photocycle by mutations in the extracellular channel or low pH (Zimanyi et al., 1992; Balashov et al., 1993; Cao et al., 1995; Brown et al., 1995; Govindjee et al. 1997), and 4) reprotonation of the chromophore is severely delayed by removal of the normal proton donor (Holz et al., 1989). These findings are readily understood in light of the present results. The torsion mechanism also allows for the possibility that the deprotonated SB carries a water molecule from the extracellular side of the active site to the intracellular side, making the pigment an inward-directed hydroxide pump rather than an outward-directed proton pump. Such a scenario is consistent with the variations in the nitrogen chemical shift of the SB through the L, M_o, M_n, and N states.

The present SSNMR results also provide insight into the recovery stage of the pump cycle. The data indicate that D85N^{neut} comprises a complex mixture of protonated SBs including *syn* C=N bonds, unlike any occurring in the WT photocycle. This disordered condition suggests that prompt deprotonation of D85 at the end of the WT photocycle is important for preventing the formation of dysfunctional C=N isomers.

We thank David Ruben and Chad Rienstra for technical assistance and Jonathan Lansing for help with NMR experiments and a careful reading of this manuscript.

This work was supported by the National Institutes of Health (GM-36810 to J.H., GM-23289 and RR-00993 to R.G.G., and NRSA GM-18962 to M.E.H.).

REFERENCES

- Balashov, S. P., R. Govindjee, M. Kono, E. Imasheva, E. Lukashev, T. G. Ebrey, R. K. Crouch, D. R. Menick, and Y. Feng. 1993. Effect of the arginine-82 to alanine mutation in bacteriorhodopsin on dark adaptation, proton release, and the photochemical cycle. *Biochemistry*. 32: 10331–10343.
- Bennett, A. E., C. M. Rienstra, M. Auger, K. V. Lakshmi, and R. G. Griffin. 1994. Heteronuclear decoupling in rotating solids. *J. Chem. Phys.* 103:6951–6958.
- Betancourt, F. M. H., and R. M. Glaeser. 2000. Chemical and physical evidence for multiple functional steps comprising the M state of the bacteriorhodopsin photocycle. *Biochim. Biophys. Acta.* 1460:106–118.
- Brown, L. S., A. K. Dioumaev, R. Needleman, and J. K. Lanyi. 1998. Local-access model for proton transfer in bacteriorhodopsin. *Biochemistry*. 37:3982–3993.
- Brown, L. S., H. Kamikubo, L. Zimanyi, L. M. Kataoka, F. Tokunaga, P. Verdegem, J. Lugtenburg, and J. K. Lanyi. 1997. A local electrostatic change is the cause of the large-scale protein conformation shift in bacteriorhodopsin. *Proc. Natl. Acad. Sci. U.S.A.* 94:5040–5044.
- Brown, L. S., J. Sasaki, H. Kandori, A. Maeda, R. Needleman, and J. K. Lanyi. 1995. Glutamic acid 204 is the terminal proton release group at the extracellular surface of bacteriorhodopsin. *J. Biol. Chem.* 270: 27122–27126.
- Cao, Y., L. S. Brown, J. Sasaki, A. Maeda, R. Needleman, and J. K. Lanyi. 1995. Relationship of proton release at the extracellular surface to deprotonation of the Schiff base in the bacteriorhodopsin photocycle. *Biophys. J.* 68:1518–1530.
- Chizhov, I., D. S. Chernavski, M. Engelhard, K.-H. Mueller., B. V. Zubov, and B. Hess. 1996. Spectrally silent transitions in the bacteriorhodopsin photocycle. *Biophys. J.* 71:2329–2345.
- de Groot, H. J. M., V. Copie, S. O. Smith, P. J. Allen, C. Winkel, J. Lugtenburg, J. Herzfeld, and R. G. Griffin. 1988. Magic-angle-sample-spinning NMR difference spectroscopy. *J. Magn. Reson.* 77:252–257.
- de Groot, H. J. M., G. S. Harbison, J. Herzfeld, and R. G. Griffin. 1989. Nuclear magnetic resonance study of the Schiff base in bacteriorhodopsin: counterion effects on the ¹⁵N shift anisotropy. *Biochemistry*. 28:3346–3353.
- de Groot, H. J. M., S. O. Smith, J. Courtin, E. van den Berg, C. Winkel, J. Lugtenburg, R. G. Griffin, and J. Herzfeld. 1990. Solid-state ¹³C and ¹⁵N study of the low pH forms of bacteriorhodopsin. *Biochemistry*. 29: 6873–6882.
- Dencher, N. A., D. Dresselhaus, G. Zaccari, and G. Buldt. 1989. Structural changes in bacteriorhodopsin during proton translocation revealed by neutron diffraction. *Proc. Natl. Acad. Sci. U.S.A.* 86:7876–7879.
- Dickopf, S., U. Alexiev, M. P. Krebs, H. Otto, R. Mollaaghbabab, H. G. Khorana, and M. P. Heyn. 1995. Proton transport by a bacteriorhodopsin mutant, aspartic acid-85 → asparagine, initiated in the unprotonated Schiff base state. *Proc. Natl. Acad. Sci. U.S.A.* 92:11519–11523.
- Engelhard, M., and B. Bechinger. 1995. Application of NMR spectroscopy to retinal proteins. *Isr. J. Chem.* 35:273–288.
- Fodor, S. P. A., J. B. Ames, R. Gebhard, E. M. M. van den Berg, W. Stoeckenius, J. Lugtenburg, and R. Mathies. 1988a. Chromophore structure in bacteriorhodopsin's N intermediate: implications for the proton-pumping mechanism. *Biochemistry*. 27:7097–7101.
- Fodor, S. P. A., W. T. Pollard, R. Gebhard, E. M. M. van den Berg, J. Lugtenburg, and R. Mathies. 1988b. Bacteriorhodopsin's L₅₅₀ intermediate contains a C14–C15 *s-trans*-retinal chromophore. *Proc. Natl. Acad. Sci. U.S.A.* 85:2156–2160.
- Friedman, N. S. Druckmann, J. Lanyi, R. Needleman, A. Lewis, M. Ottolenghi, and M. Sheves. 1994. A covalent link between the chromophore and the protein backbone of bacteriorhodopsin is not required for forming a photochemically active pigment analogous to the wild type. *Biochemistry*. 33:1971–1976.
- Gat, Y., and M. Sheves. 1994. The origin of the red-shifted absorption maximum of the M₄₁₂ intermediate in the bacteriorhodopsin photocycle. *Photochem. Photobiol.* 59:371–378.
- Gochnauer, M. B., and D. J. Kushner. 1969. Growth and nutrition of extremely halophilic bacteria. *Can. J. Microbiol.* 15:1157–1165.
- Govindjee, R., E. S. Imasheva, S. Misra, S. P. Balashov, T. G. Ebrey, N. Chen, D. R. Menick, and R. Crouch. 1997. Mutation of a surface residue, lysine-129, reverses the order of proton release and uptake in bacteriorhodopsin; guanidine hydrochloride restores it. *Biophys. J.* 72: 886–898.
- Han, B.-G., J. Vonck, and R. M. Glaeser. 1994. The bacteriorhodopsin photocycle: direct structural study of two substates of M-intermediate. *Biophys. J.* 67:1179–1186.

- Harbison, G. S., J. Herzfeld, and R. G. Griffin. 1983. Solid-state nitrogen-15 nuclear magnetic resonance study of the Schiff base in bacteriorhodopsin. *Biochemistry*. 22:1–5.
- Harbison, G. S., S. O. Smith, J. A. Pardo, J. M. L. Courtin, J. Lugtenburg, J. Herzfeld, R. A. Mathies, and R. G. Griffin. 1985. Solid-state ^{13}C NMR detection of a perturbed 6-*s-trans* chromophore in bacteriorhodopsin. *Biochemistry*. 24:6955–6962.
- Harbison, G. S., S. O. Smith, J. A. Pardo, P. P. J. Mulder, J. Lugtenburg, J. Herzfeld, R. Mathies, and R. G. Griffin. 1984a. Solid-state ^{13}C NMR studies of retinal in bacteriorhodopsin. *Biochemistry*. 23:2662–2667.
- Harbison, G. S., S. O. Smith, J. A. Pardo, C. Winkel, J. Lugtenburg, J. Herzfeld, R. Mathies, and R. G. Griffin. 1984b. Dark-adapted bacteriorhodopsin contains 13-*cis*,15-*syn* and all-*trans*,15-*anti* retinal Schiff bases. *Proc. Natl. Acad. Sci. U.S.A.* 81:1706–1709.
- Haupt, U., J. Tittor, and D. Oesterhelt. 1999. Closing in on bacteriorhodopsin: progress in understanding the molecule. *Annu. Rev. Biophys. Biomol. Struct.* 28:367–399.
- Herome, A., and K. Kuczera. 1998. Free-energy simulations of the retinal *cis*→*trans* isomerization in bacteriorhodopsin. *Biochemistry*. 37:2843–2853.
- Herzfeld, J., and J. G. Hu. 1996. Bacteriorhodopsin and rhodopsin. *Encycl. NMR*. 2:862–871.
- Herzfeld, J., and J. C. Lansing. 2002. Magnetic resonance studies of the bacteriorhodopsin pump cycle. *Annu. Rev. Biophys. Biomol. Struct.* In press.
- Herzfeld, J., and B. A. Tounge. 2000. NMR Probes of vectoriality in the proton-motive photocycle of bacteriorhodopsin: evidence for an electrostatic steering mechanism. *Biochim. Biophys. Acta. Bioenerg.* 1460:95–105.
- Holz, M. L. A. Drachev, T. Mogi, H. Otto, A. D. Kaulen, M. P. Heyn, V. P. Skulachev, and H. G. Khorana. 1989. Replacement of aspartic acid-96 by asparagine in bacteriorhodopsin slows both the decay of the M intermediate and the associated proton movement. *Proc. Natl. Acad. Sci. U.S.A.* 86:2167–2171.
- Hu, J. G., R. G. Griffin, and J. Herzfeld. 1994. Synergy in the spectral tuning of retinal pigments: complete accounting of the opsin shift in bacteriorhodopsin. *Proc. Natl. Acad. Sci. U.S.A.* 91:8880–8884.
- Hu, J. G., R. G. Griffin, and J. Herzfeld. 1997a. Interaction between the protonated Schiff base and its counterion in the photointermediates of bacteriorhodopsin. *J. Am. Chem. Soc.* 119:9495–9498.
- Hu, J. G., B. Q. Sun, M. Bizounok, M. E. Hatcher, J. C. Lansing, J. Raap, P. J. E. Verdegem, J. Lugtenburg, R. G. Griffin, and J. Herzfeld. 1998. Early and late M photointermediates in the bacteriorhodopsin photocycle: a solid state NMR study. *Biochemistry*. 37:8088–8096.
- Hu, J. G., B. Q. Sun, A. T. Petkova, R. G. Griffin, and J. Herzfeld. 1997b. The pre-discharge chromophore in bacteriorhodopsin: a ^{15}N solid state study of the L-photointermediate. *Biochemistry*. 36:9316–9322.
- Kataoka, M., H. Kamikubo, F. Tokunaga, L. S. Brown, Y. Yamazaki, A. Maeda, M. Sheves, R. Needleman, and J. K. Lanyi. 1994. Energy coupling in an ion pump: the reprotonation switch of bacteriorhodopsin. *J. Mol. Biol.* 243:621–638.
- Lakshmi, K. V., M. R. Farrar, J. Raap, J. Lugtenburg, R. G. Griffin, and J. Herzfeld. 1994. Solid state ^{13}C and ^{15}N NMR investigation of the N intermediate of bacteriorhodopsin. *Biochemistry*. 33:8853–8857.
- Lansing, J. C., M. Hohwy, C. P. Jaroniec, A. F. L. Creemers, J. Lugtenburg, J. Herzfeld, and R. G. Griffin. 2002. Chromophore distortions in the bacteriorhodopsin photocycle: evolution of the H-C14–C15-H dihedral angle measured by solid-state NMR. *Biochemistry*. In press.
- Lanyi, J. K. 1998. Understanding structure and function in the light-driven proton pump bacteriorhodopsin. *J. Struct. Biol.* 124:164–178.
- Ludmann, K., C. Gergely, and G. Varo. 1998. Kinetic and thermodynamic study of the bacteriorhodopsin photocycle over a wide pH range. *Biophys. J.* 75:3110–3119.
- Luecke, H. 2000. Atomic resolution structures of bacteriorhodopsin photocycle intermediates: the role of discrete water molecules in the function of this light-driven ion pump. *Biochim. Biophys. Acta.* 1460:133–56.
- Marti, T., J. Otto, T. Mogi, S. Rosselet, M. Heyn, and G. Khorana. 1991. The retinylidene Schiff base counterion in bacteriorhodopsin. *J. Biol. Chem.* 266:18674–18683.
- Mathies, R. A., and X.-Y. Li. 1995. On modeling the vibrational spectra of 14-*s-cis* retinal conformers in bacteriorhodopsin. *Biophys. Chem.* 56:47–55.
- Mogi, T., L. J. Stern, T. Marti, B. H. Chao, and H. G. Khorana. 1988. Aspartic acid substitutions affect proton translocation by bacteriorhodopsin. *Proc. Natl. Acad. Sci. U.S.A.* 85:4148–4152.
- Moltke, S., and M. P. Heyn. 1995a. Photovoltage kinetics of the acid-blue and acid-purple forms of bacteriorhodopsin: evidence for no net charge transfer. *Biophys. J.* 69:2066–2073.
- Moltke, S., M. P. Krebs, R. Mollaaghbabaa, H. G. Khorana, and M. P. Heyn. 1995b. Intramolecular charge transfer in the bacteriorhodopsin mutants Asp85→Asn and Asp212→Asn: effects of pH and anions. *Biophys. J.* 69:2074–2083.
- Needleman, R., M. Chang, B. Ni, G. Varo, J. Fornes, S. H. White, and J. K. Lanyi. 1991. Properties of Asp212→Asn bacteriorhodopsin suggest that Asp212 and Asp85 both participate in a counterion and proton acceptor complex near the Schiff base. *J. Biol. Chem.* 266:11478–11484.
- Oesterhelt, D., and W. Stoerkenius. 1974. Isolation of the cell membrane of *Halobacterium halobium* and its fractionation into red and purple membrane. *Methods Enzymol.* 31:667–678.
- Otto, H., T. Marti, M. Holz, T. Mogi, L. J. Stern, F. Engel, H. G. Khorana, and M. P. Heyn. 1990. Substitution of amino acids Asp-85, Asp-212 and Arg-82 in bacteriorhodopsin affects the proton release phase of the pump and the pK of the Schiff base. *Proc. Natl. Acad. Sci. U.S.A.* 87:1018–1022.
- Pardo, J. A., P. P. J. Mulder, E. M. M. van den Berg, and J. Lugtenburg. 1985. Synthesis of 8-mono- ^{13}C -retinal, 9-mono- ^{15}C -retinal, 12-mono- ^{13}C -retinal and 13-mono- ^{13}C -retinal. *Can. J. Chem.* 63:1431–1435.
- Pardo, J. A., C. Winkel, P. P. J. Mulder, and J. Lugtenburg. 1984. Synthesis of retinals labeled at positions 14 and 15 (with ^{13}C and/or ^2H). *Recl. Trav. Chim. Pays Bas.* 103:135–141.
- Radionov, A. N., V. A. Klyachko, and A. D. Kaulen. 1999. Formation of the M-N (M-open) intermediate in the wild-type bacteriorhodopsin photocycle is accompanied by an absorption spectrum shift to shorter wavelength, like that in the mutant D96N bacteriorhodopsin photocycle. *Biochem. (Moscow)*. 64:1210–1214.
- Rothschild, K. S., M. S. Braiman, Y. W. He, T. Marti, and H. G. Khorana. 1990. Vibrational spectroscopy of bacteriorhodopsin mutants. Evidence for the interaction of aspartic acid 212 with tyrosine 185 and possible role in the proton pump mechanism. *J. Biol. Chem.* 265:16985–16991.
- Sass, H. J., I. W. Schachowa, G. Raap, M. H. J. Koch, D. Oesterhelt, N. A. Dencher, and G. Bueldt. 1997. The tertiary structural changes in bacteriorhodopsin occur between M states: x-ray diffraction and Fourier transform infrared spectroscopy. *EMBO J.* 16:1484–1491.
- Scharnagle, C., J. Hettenkofer, and S. F. Fisher. 1995. Electrostatic and conformational effects on the proton translocation steps in bacteriorhodopsin: analysis of multiple M structures. *J. Phys. Chem.* 99:7787–7800.
- Schulten, K., and P. Tavan. 1978. A mechanism for the light-driven proton pump of *Halobacterium halobium*. *Nature*. 272:85–86.
- Schweiger, U., J. Tittor, and D. Oesterhelt. 1994. Bacteriorhodopsin can function without a covalent linkage between retinal and protein. *Biochemistry*. 33:535–541.
- Smith, S. O., H. J. M. DeGroot, R. Gebhard, J. M. L. Courtin, J. Lugtenburg, J. Herzfeld, and R. G. Griffin. 1989. Structure and protein environment of the retinal chromophore in light- and dark-adapted bacteriorhodopsin studied by solid-state NMR. *Biochemistry*. 28:8897–8904.
- Smith, S. O., Lugtenburg, J., and R. Mathies. 1985. Determination of retinal chromophore structure in bacteriorhodopsin with resonance Raman spectroscopy. *J. Membr. Biol.* 85:95–109.
- Smith, S. O., and R. Mathies. 1985. Resonance Raman spectra of the acidified and deionized forms of bacteriorhodopsin. *Biophys. J.* 47:251–254.
- Smith, S. O., J. A. Pardo, P. J. Mulder, B. Curry, J. Lugtenburg, and R. Mathies. 1983. Chromophore structure in bacteriorhodopsin's O_{640} photointermediate. *Biochemistry*. 22:6141–6148.

- Song, L., M. A. El-Sayed, and J. K. Lanyi. 1996. Effect of changing the position and orientation of Asp85 relative to the protonated Schiff base within the retinal cavity on the rate of photoisomerization in bacteriorhodopsin. *J. Phys. Chem.* 100:10479–10481.
- Song, L., D. Yang, M. A. El-Sayed, and J. K. Lanyi. 1995. Retinal isomer composition in some bacteriorhodopsin mutants under light and dark adaptation conditions. *J. Phys. Chem.* 99:10052–10055.
- Subramaniam, S. 1999. The structure of bacteriorhodopsin: an emerging consensus. *Curr. Opin. Struct. Biol.* 9:462–468.
- Subramaniam, S., M. Gerstein, D. Oesterhelt, and R. Henderson. 1993. Electron diffraction analysis of structural changes in the photocycle of bacteriorhodopsin. *EMBO J.* 12:1–8.
- Subramaniam, S., I. Lindahl, P. Bullough, A. R. Faruqi, J. Tittor, D. Oesterhelt, L. Brown, J. Lanyi, and R. Henderson. 1999. Protein conformational changes in the bacteriorhodopsin photocycle. *J. Mol. Biol.* 287:145–161.
- Tittor, J., S. Paula, S. Subramaniam, J. Heberle, R. Henderson, and D. Oesterhelt. 2000. Bacteriorhodopsin can translocate protons without a significant conformational change. *Biophys. J.* 78:478A.
- Turner, G. J., L. J. W. Miercke, T. E. Thorgerisson, D. S. Kliger, M. C. Betlach, and R. M. Stroud. 1993. Bacteriorhodopsin D85N: three spectroscopic species in equilibrium. *Biochemistry.* 32:1332–1337.
- Vonck, J., B. G. Han, F. Burkard, G. A. Perkins, and R. M. Glaeser. 1994. Progressive substates of the M-intermediate can be identified in glucose-embedded, wild-type bacteriorhodopsin. *Biophys. J.* 67:1173–1178.
- Yoshida, M., K. Ohno, and Y. Takeuchi. 1980. Altered activity of bacteriorhodopsin in high concentrations of guanidine hydrochloride. *J. Biochem.* 87:491–495.
- Yoshida, M., K. Ohno, Y. Takeuchi, and Y. Kagawa. 1977. Prolonged lifetime of the 410-nm intermediate of bacteriorhodopsin in the presence of guanidine hydrochloride. *Biochem. Biophys. Res. Commun.* 75:1111–1116.
- Zhou, F., A. Windemuth, and K. Schulten. 1993. Molecular dynamics study of the proton pump cycle of bacteriorhodopsin. *Biochemistry.* 32:2291–2306.
- Zimanyi, L., G. Varo, M. Chang, B. Ni, R. Needleman, and J. K. Lanyi. 1992. Pathways of proton release in the bacteriorhodopsin photocycle. *Biochemistry.* 31:8535–8543.